Available online at www.eccomasproceedia.org
Eccomas Proceedia SMART (2023) 454-464

ECCOMAS
Proceedia

X ECCOMAS Thematic Conference on Smart Structures and Materials
SMART 2023
D.A. Saravanos, A. Benjeddou, N. Chrysochoidis and T. Theodosiou (Eds)

DESIGN AND OPTIMIZATION OF A SELF-EXPANDABLE NITI BRAIDED STENT USING MOPSO ALGORITHM

SEYEDEH FARZANEH HOSEINI*, ANDREA SPAGGIARI†

* Dipartimento di Scienze e Metodi dell'Ingegneria
Università di Modena e Reggio Emilia
e-mail: 311596@studenti.unimore.it

† Dipartimento di Scienze e Metodi dell'Ingegneria
Università di Modena e Reggio Emilia
e-mail: andrea.spaggiari@unimore.it

Abstract. Cardiovascular stents are indispensable medical devices used to treat vessel-related issues such as atherosclerotic plaque. In the past, stents were mainly made of materials like stainless steel or cobalt-chromium alloy. However, over the last two decades, research has focused on the use of Nitinol (NiTi) due to its superior properties such as super-elasticity, biocompatibility, and strength. The aim of this paper is to optimize the design of the open-ended braided stent, a well-known architecture for endovascular stents, subjected to radial compression, for enhanced performance. The optimization process uses Multi-Objective Particle Swarm Optimization (MOPSO), which explores three design variables, namely wire diameter, number of coils, and pitch angle, to determine the optimal shape that maximizes radial pressure stiffness and radial force exerted on the vessel walls while minimizing foreshortening. The analytical model developed is compared against literature findings, and the optimization results are implemented in a finite element analysis solver and compared with existing references. The study finds that the optimized design using MOPSO improves the mechanical performance of the stent, particularly in terms of radial stiffness. The results demonstrate the feasibility of MOPSO for optimizing braided NiTi stents and the use of FEM for validating optimized designs. The work emphasizes the significance of optimizing the design of cardiovascular stents to enhance their performance and assure their effectiveness in treating artery diseases.

Key words: Self-expanding braided stent, NiTi, optimization, MOPSO algorithm, FEM

1 INTRODUCTION

The word "stent" was first used in the context of medical devices in the mid-20th century. It is named after a British dentist, Dr. Charles T. Stent, who contributed to the development of materials used in making early medical devices [1]. Cardiovascular stents are critical medical devices used in the treatment of artery diseases, such as atherosclerotic plaque. Stents are designed to maintain vessel patency and prevent restenosis by providing mechanical support to the artery walls [2] . Stent materials made of metal can be classified into various types based on their composition, such as Nitinol, stainless steel, cobalt-chromium, and other

Peer-review under responsibility of the organizing committee of SMART 2023.
doi: 10.7712/150123.9800.449429

metallic alloys. Metallic material consists of Nitinol, stainless steel, cobalt-chromium, and other metallic alloys. Stainless steel and cobalt-chromium alloy were commonly used materials for stents in the past. However, over the last two decades, the focus has shifted towards using Nitinol (NiTi) which is a type of Shape Memory Alloys (SMAs) [1]–[3] . SMAs are a class of smart materials that have the ability to remember and recover their initial shape when exposed to thermal or mechanical loads. Among all SMAs, NiTi is the most widely used one because of its superior properties like super-elasticity, biocompatibility, flexibility, outstanding functional stability, good wear and corrosion resistance, and fair resistance to fatigue [4]. The category of metallic stents is additionally subdivided into two expansion methods: balloon-expandable and self-expanding (SX). Balloon-expandable stents are expanded using a pressurized balloon, while self-expanding stents, such as braided SX stents, rely on an elastic springback to expand after the contraction needed for the insertion. The SX stent is resilient enough to recover its original shape after being unloaded from extreme deformations [5], [6].

In this study, we focus on braided SX stents. Braided stents are typically made of a metal alloy, such as Nitinol, and consist of a series of interwoven wires that can expand and contract like a spring. Braided SX stents offer several advantages in the treatment of vascular disease. These stents are highly flexible and adaptable, allowing them to conform to the complex shapes of vessels and reduce the risk of injury or complications. Their kink resistance helps to prevent collapse or damage during deployment, and their flexible design causes less damage to the vessel wall, reducing the risk of restenosis or thrombosis [7]–[13].

In addition to the importance of the materials used to manufacture stents, evaluating the structure and geometry of stents are also crucial. In 1993 Michael R. Jedwab et.al [14] presented a mathematical model of an open-end self-expanding braided stent to describe both mechanical and geometrical properties of the stent and finally, they validated their model by conducting several experimental tests on a sample stent. In 2017, Shanahan et al. [15] investigated whether the formula proposed by Jedwab and Clerc [14] can be used to predict the mechanical behavior of looped-end braided stent designs. For this purpose, they studied two stent designs, open-end braided and looped-end braided stents, with the same materials and initial geometry parameters. They found that the suggested analytical model is not completely applicable for modeling the looped-end designs' mechanical behavior and the magnitude of radial force and peak stress in the looped-ends can only be predicted by the FE Model. Chen Pan et al. in their recent review [16] analyzed different stent structural designs. Three different types of stents including the bridging, representative volume element (RVE)/representative unit cell (RUC), and patient-specific stents were examined for mechanical properties such as radial stiffness, foreshortening, and axial flexibility. They studied the structural challenges of existing stents and listed mechanical pros and cons for various structural designs. Based on their study, achieving a balance between high radial stiffness and axial flexibility is a crucial standard and challenging design problem for stents, emphasizing the necessity to optimize stent designs.

There are several factors that can be considered when optimizing braided stents, such as the material used, the design of the braid, the size and shape of the stent, and the coating applied to the stent. The goal of optimizing a braided stent is typically to improve its performance, such as increasing its flexibility, strength, and resistance to damage, while also reducing its cost and complexity. This can be done through a combination of material selection, design,

manufacturing techniques, and an optimization algorithm such as the Multi-Objective Particle Swarm Optimization (MOPSO) algorithm. MOPSO is a powerful optimization technique that can efficiently explore the design space of the braided stent and identify the optimal design that meets the desired mechanical properties.
The aim of this study is to improve the mechanical properties of the braided stent when it's fully deployed in the vessel using an optimization algorithm. In the first step, the mechanical properties of a braided stent structure through an analytical model proposed by Jedwab et. al [14] are investigated. Then, to improve the mechanical properties of the stent when it is fully deployed in the vessel, its mechanical behavior using the analytical model and FE model was verified with the literature [15]. Finally, to find the optimized structural design, the Multi-Objective Particle Swarm Optimization (MOPSO) algorithm [17] was utilized by focusing on maximizing radial pressure stiffness and radial force and minimizing the maximum stent length under periodic pressure from the vessel.

2 MATERIALS AND METHODS

In the following paragraphs, a detailed description of an analytical model, based on Jedwab's approach [14], is presented to predict the mechanical behavior of an open-ended braided stent, including radial force and stiffness. To improve the mechanical performance of the stent, optimizing the stent design using the MOPSO algorithm is explored. To validate our results, a radial compression test is simulated by means of a nonlinear finite element analysis of the stent in contact with the crimper.

2.1 Material selection

All stents, regardless of the method of deployment used, are implantable medical devices, so they are required to exhibit high levels of biocompatibility as well as resistance to corrosion. They should have high radiopacity and produce very little interference when used in MRI machines. The second reason biocompatibility is important is that corrosion results in the release of metallic ions inside the body. The ideal material for an SX stent would also have a low elastic modulus but a high yield stress, making it both flexible and resistant to fracture [15]. Over the years, stent materials and designs have evolved significantly to enhance their efficacy and minimize the risks associated with their use. Compared to other materials, Nitinol, a Nickel-Titanium (NiTi) shape memory alloy meets the majority of stent design requirements because of its special characteristics and excellent behavior such as flexibility, non-magnetic, recoverability from large deformation, excellent biocompatibility, and high corrosion resistance [18], [19]. Therefore, in this work, the behavior of a NiTi-based self-expanding braided stent is investigated.

2.2 Cylindrical braided stent

The braided stent is a kind of self-expanding design composed of two sets of interlacing wires twisted in a helical route along the stent axis in two opposite directions, clockwise and counterclockwise, as shown in Figure 1. The aim of the model is to estimate the geometry and mechanical characteristics of a self-expanding open-ended braided stent under the action of axial load F and radial pressure P. In the following section, the analytical formulae suggested by Jedwab and Clerc [14] are summarized.

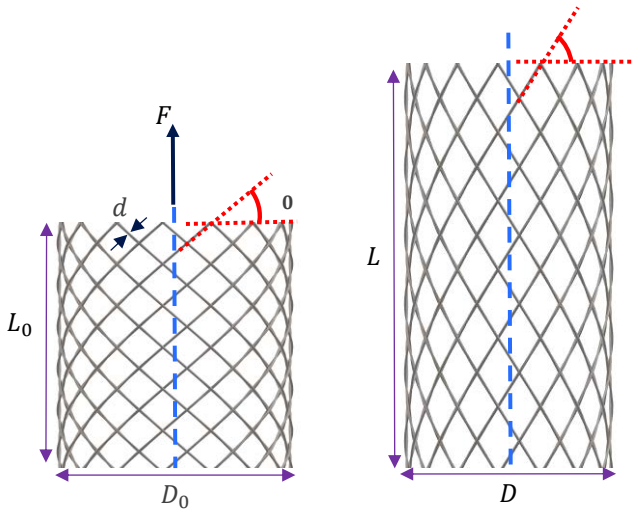

Figure 1: Stent elongation under axial loading F

2.2.1 Stent geometry

The parameters of the braided stent (see Figure 1) are the initial stent diameter D_0, the initial length of the stent L_0, the diameter of the wires d, the number of wires N, and the initial pitch/braided angle β_0. The pitch angle is the angle between any helix and the circumferential axis. When an axial load F is applied on the stent, the braided angle will increase from β_0 to β. At the same time, the initial stent's length extends to a new length L, while its initial diameter reduces to D. Using these parameters, the initial pitch p_0 and the number of coils c are given by the following equations.

$$p_0 = \pi D_0 tan\beta_0 \tag{1}$$

$$c = {}^{L_0}/_{P_0} \tag{2}$$

Based on the assumption that the length of the wires stays constant, the relationships between the ultimate length L and the diameter D and the pitch angle are as follows:

$$D = \frac{D_0 cos\ (\ )}{cos\ (\ _0)} \tag{3}$$

$$L = \frac{L_0 sin\ (\ )}{sin\ (\beta_0)} \tag{4}$$

Equation (5) also computes the minimum pitch angle $_{min}$ associated with the maximum compressed configuration [20].

$$_{min} = arctan\left(\frac{dN}{\pi D}\right) \tag{5}$$

2.2.2 Mechanical properties

The stent model is based on the assumption that the behaviour is similar to a collection of independent open-coiled helical springs. It is assumed that 1) the stent undergoes only elastic deformation, and 2) the stent's ends are fixed against rotating around the longitudinal axis

because of the friction between the wires at their crossing points. Assuming the stent is subjected to a tension test, the axial force F exerted on the stent may be calculated using the following equation [20].

$$= 2N\left[\frac{GI_P}{K_3}\left(\frac{2sin(\ )}{K_3} - K_1\right) - \frac{EItan(\beta)}{K_3}\left(\frac{2cos(\beta)}{K_3} - K_2\right)\right] \tag{6}$$

Where K_1, K_2, and K_3 are constants as follow:

$$K_1 = \frac{sin(2\ _0)}{D_0} \qquad K_2 = \frac{2cos^2(\beta_0)}{D_0} \qquad K_3 = \frac{D_0}{cos(\beta_0)} \tag{7}$$

$I$and I_P represent the moment of inertia and polar moment of inertia, respectively, and G and E are the shear modulus and Young's modulus respectively. The work done by load F is by definition $dW=Fd\delta$. The same deflection δ can be generated by applying a uniformly distributed radial pressure P to an imaginary lateral surface πDL around the stent. The work done by the pressure P is equal to:

$$dW = P\pi DL\frac{dD}{2} \tag{8}$$

As P and perform an equal amount of work, the pressure required to achieve the same deflection in a stent can be computed as follows:

$$P = \frac{2Fc}{DLtan(\beta)} \tag{9}$$

Therefore, the radial force $_R$ can be calculated as follows.

$$_R = \frac{2\pi Fc}{tan(\ )} \tag{10}$$

To calculate the radial pressure stiffness K_P, the following equation is found in [20].

$$K_P = \frac{2c}{K_3\sin(\beta)\left(DLtan(\beta)\right)^2} \times \left[\begin{array}{c} 2DLN.\tan(\beta)\left(\frac{GI_p}{K_3}\left(\frac{2\cos(\beta)}{K_3}\right) - \frac{EI}{K_3}\left(\frac{2\cos(\ )}{K_3} - \frac{K_2}{cos^2(\beta)}\right)\right) \\ -F\left(\frac{DL}{cos^2(\beta)} + K_3\sin(\beta) \times (\pi cD - L.\tan(\beta))\right) \end{array}\right] \tag{11}$$

Considering one of the open-coiled helical springs under the action of the load F, the bending and twisting moments (σ, τ) are given as follows.

$$\sigma = \frac{/_N sin(\beta).{}^D/_2 . d}{I} \qquad \tau = \frac{/_N cos(\beta).{}^D/_2 . d}{I_p} \tag{12}$$

According to distortion energy, the equivalent Von Mises' stress σ_e is a function of shear stress τ and bending stress σ as follows:

$$\sigma_e = \sqrt{\sigma^2 + 3\tau^2} = \frac{8FD}{N\pi d^3}\sqrt{4sin^2\ \ + 3cos^2} \tag{13}$$

2.3 Optimization

An optimal stent, in addition to having sufficient flexibility against pulses, should have a

considerable radial force and radial stiffness [21] to maintain the vessels open. In addition, foreshortening is an important parameter to consider when optimizing stents, since it can affect the performance and function of the stent. Foreshortening refers to the degree to which a stent is compressed along its longitudinal axis, which can occur during the deployment of the stent, as it expands radially. Although braided stents provide high coverage and flexibility, they significantly shorten after expansion, which leads to the stent being displaced from its position and decreasing the treatment's outcome [18]. Therefore, the geometrical design should be such that a change in the diameter value of the stent does not result in a substantial change in axial length.

In this study, we used the Multi-Objective Particle Swarm Optimization (MOPSO) algorithm in Matlab to optimize the stent design. The MOPSO algorithm is a metaheuristic optimization algorithm that works by simulating a swarm of particles moving in a search space to find optimal solutions [17]. We aimed to maximize the radial force, F_R and radial stiffness K_P of the stent while minimizing the length variation of the stent under axial loading L_{max}, to avoid foreshortening. To achieve an efficient stent, we used the MOPSO algorithm to explore three design variables, namely wire diameter (d), number of coils (N), and pitch angle (β_0). The following ranges of d, N, β_0 are specified.

$$0.1\ mm \leq d \leq 0.30mm \tag{14}$$

$$10 \leq N \leq 40$$

$$_{min} \leq \ _0 \leq 70°$$

Moreover, we imposed constraints on the maximum Von Mises stress and volume of the optimal designed stent in order to permit a fair comparison between the optimized design and the reference design [15].

$$\sigma_e \leq yield\ stress \tag{15}$$

$$Volume_{opt} \leq Volume_{ref}$$

2.3.1 Optimization parameters

The algorithm has several parameters that can be adjusted to influence its performance. In our study, we used a population size of 100 particles, and the maximum number of iterations is set to 200. We used a repository size of 100 particles, and 30 divisions for the adaptive grid. The values of the mutation rate and the global learning coefficients were set to 0.5, 1, and 2, respectively. These parameter values were chosen based on default values presented in the reference [17] that have shown their effectiveness in optimizing different problems. By fine-tuning these parameters, we were able to effectively explore the search space and find a set of stent designs that fulfill multiple objectives simultaneously.

2.4 Numerical simulation

To verify the accuracy of the results obtained from the numerical analysis and gain a deeper understanding of the mechanical behavior of stents during the crimping process, finite

element analysis simulations are conducted. The stent's geometry is designed using Solidworks software, utilizing the initial geometrical parameters, including pitch angle (β_0), number of wires (N), the diameter of wires (d), and initial length (L_0) and diameter (D_0) of the stent. The generated geometry is imported into Abaqus/CAE version 6.14 using the STEP format, providing the required framework for finite element analysis (FEA). To analyze the stent's mechanical behavior, the geometry has meshed with 2-node linear beam elements (B31), which allows us to have both an excellent computational efficiency and good accuracy of the responses. To model the contact between the braiding wires at the intersection points, we employed JOIN connectors, without friction. These elements are used to simulate the rotational behavior of wires at the intersection points by linking the two opposing nodes, allowing for unrestricted rotation around the intersection points, as already suggested in [22].
To accurately simulate the stent crimping process, a model of the crimper is exploited. The crimper is modeled as a cylindrical shell, type surface in Abaqus, and meshed using a 4-node quadrilateral surface element, reduced integration (SFM3D4R). The inner surface of the crimper is also designated as a set to define the contact between the stent and the crimper during compression simulation.

2.4.1 Radial compression simulation

To accurately simulate the radial compression on the stent, a radial displacement is imposed on the crimper in cylindrical coordinates. Figure 2 shows the initial configuration of the simulation model. A frictionless surface-to-surface contact is then defined between the inner surface of the crimper and the outer node set of the stent. Additionally, to axially constrain the end of the stent, a displacement boundary condition is applied to the corresponding nodes. The stent is in Nitinol, modeled as a linear material with an austenitic Young's modulus of 35.9 GPa, and Poisson's ratio of 0.33. Since the focus is on predicting the radial force on the stent wall at full deployment with approximately 40% global crimping, it is possible to assume that local stress stays within the linear elastic region, as the local deformation is fairly low.

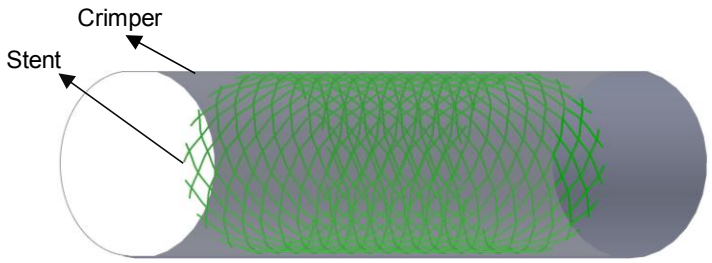

Figure 2: Model of the crimper and stent in the initial configuration

3 RESULTS AND DISCUSSION

3.1 Validation of the analytical results

To validate the analytical results of our model, we designed a stent based on previous research conducted by Shanahan [15] and then applied a radial displacement by means of the crimper surface to reduce the stent's external diameter from 22 mm to 10 mm ($D_0 \rightarrow D$), as it was

done in the reference. The design parameters for the stent and the characteristics of the finite element (FE) model are presented in Table 1. By utilizing the FE model, we conducted a comparative analysis between our results and the reference data. This approach enabled us to verify the accuracy of our analytical model and demonstrate its effectiveness in predicting the behavior of the stent. As illustrated in Figure 3, the analytical model demonstrates excellent agreement with the reference data for the length, radial force, and stress parameters. Furthermore, the simulation results indicate strong agreement between the analytical and simulated values for stent length. While the radial force values display a similar trend, there is a slight discrepancy in the numerical values. This difference could be due to the boundary condition given to the end nodes of the stent. Moreover, the von Mises stress values also align well with the analytical data. Additionally, our simulation results show that the maximum stress in the stent is around 135 MPa (as shown in Figure 4), which is in excellent agreement with the analytically derived maximum stress of approximately 130 MPa. These stress values support the linear model chosen for the material since the strain in the global stent is around 3%. This strong agreement further supports the validity of our model in predicting stent behavior. The findings suggest that the analytical and simulation models are effective tools for predicting stent behavior and designing optimized geometry of the stent.

Table 1: Design parameters for the stent and crimper, and characteristics of the finite element model

Parameters	Stent	Crimper
Initial external diameter D_0 (mm)	22	22.1
Final external diameter D_0 (mm)	10	10
Wire diameter d (mm)	0.22	-
Initial length L_0 (mm)	53.56	100
Initial branding angle β_0 (°)	30	-
Number of wires N	30	-
Finite element type	B13	SFM3D4R

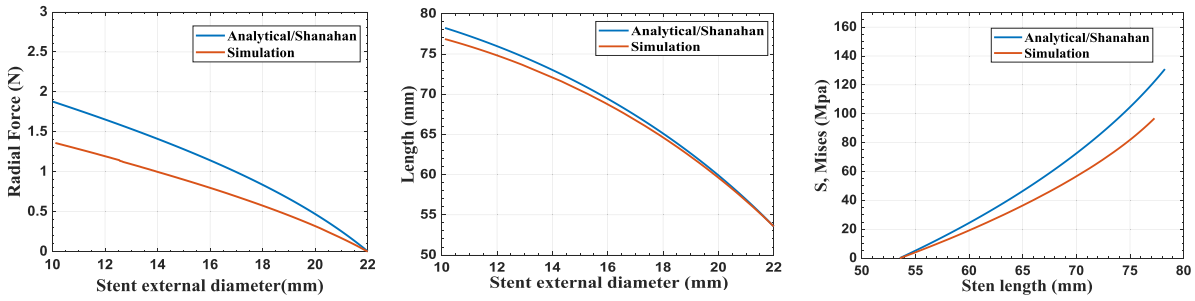

(a) (b) (c)

Figure 3: Comparison between the analytical and simulation results with the reference: a) radial force versus the stent external diameter b) the length of the stent versus the stent external diameter and c) equivalent Von-Mises stress versus the length of the stent

3.2 Optimized design

In accordance with the guidelines outlined in section 2.3, the stent design was optimized using the Multi-Objective Particle Swarm Optimization (MOPSO) technique. Our primary objective was to increase both radial force and radial stiffness while simultaneously reducing the length variation under axial loading. Through an iterative process of optimization, three design parameters are explored: wire diameter, number of coils, and pitch angle. To ensure a meaningful comparison between the optimized and reference designs, constraints were set on both the volume of the stent and the maximum Von Mises stress. The optimized design parameters obtained through this process are presented in Table 2, while the analytical results of the optimization process are summarized in Figure 5.

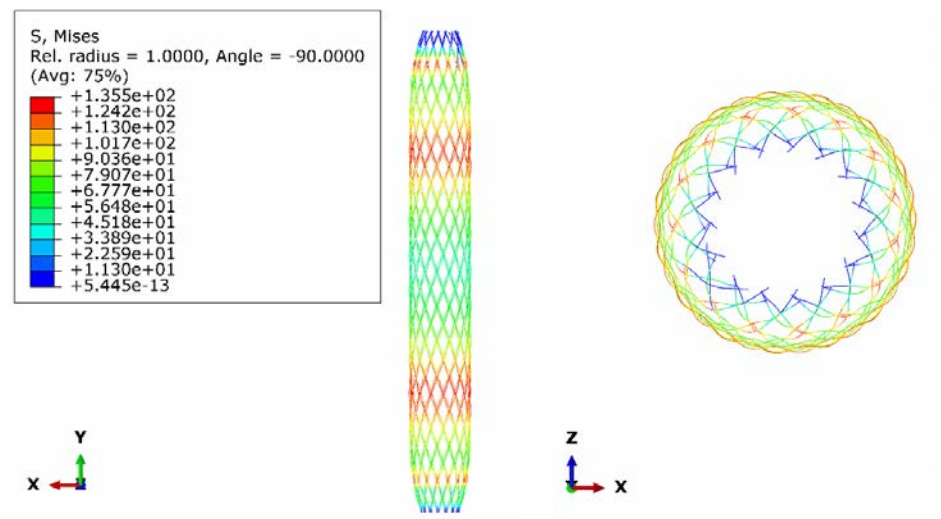

(a) (b)

Figure 4: Von Mises stress distribution under uniform radial compression; a) front view b) top view

The optimized stent design shows a maximum radial force of 2.6 N and a maximum radial stiffness of 0.18 N/mm; these figures represent a 38% and 52% improvement, respectively, over the reference design. In addition, the length variation of the optimized stent was reduced by 4.5% compared to the reference design, indicating improved accuracy in stent deployment. These findings show that the MOPSO algorithm is capable of optimizing stent design, thereby improving stent performance and enhancing clinical outcomes for patients.

Table 2: Optimized design parameters

Initial branding angle β_0 (°)	Number of wires N	Wire diameter d (mm)
42.55	16	0.29

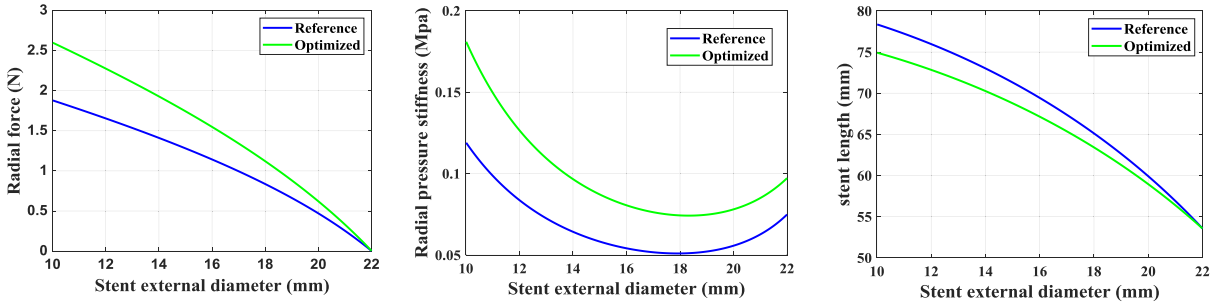

(a) (b) (c)

Figure 5: Analytical comparison between the optimized stent design and the reference design; a) radial force versus stent external diameter b) radial pressure stiffness versus stent external diameter c) stent length versus stent external diameter

4 CONCLUSION

This paper describes a comprehensive study of the design and optimization of a stent using analytical and simulation models. The analytical model was first validated by comparing the results with reference data obtained from a previous study using FEA. The comparison showed excellent agreement between the analytical model and the reference data in terms of stent length, radial force, and stress parameters. Subsequently, Multi-Objective Particle Swarm Optimization (MOPSO) was used to improve the stent design by exploring three important design variables: wire diameter, number of coils, and pitch angle. The objective of the optimization procedure was to improve the radial stiffness and radial force of the stent while minimizing the length variation of the stent under loading. In comparison to the reference design, our findings show that the optimized design significantly boosts the stent's mechanical performance by 38% in terms of radial force and 52% in terms of radial stiffness. In addition, the length variation of the optimized stent was decreased by 4.5%, demonstrating enhanced stent deployment precision. Overall, the analytical and simulation models created in this study demonstrated to be highly effective at predicting stent behavior and designing an optimum stent geometry, which may enhance device performance.

REFERENCES

[1] I. Ohkata, *Medical applications of superelastic nickel-titanium (Ni–Ti) alloys*. Woodhead Publishing Limited, 2011.

[2] M. Ullah *et al.*, “Stent as a Novel Technology for Coronary Artery Disease and Their Clinical Manifestation,” *Curr. Probl. Cardiol.*, vol. 48, no. 1, p. 101415, 2023, doi: 10.1016/j.cpcardiol.2022.101415.

[3] M. H. Elahinia, M. Hashemi, M. Tabesh, and S. B. Bhaduri, “Manufacturing and processing of NiTi implants: A review,” *Prog. Mater. Sci.*, vol. 57, no. 5, pp. 911–946, 2012, doi: 10.1016/j.pmatsci.2011.11.001.

[4] N. Farjam, M. Nematollahi, M. T. Andani, M. J. Mahtabi, and M. Elahinia, “Effects of size and geometry on the thermomechanical properties of additively manufactured NiTi shape memory alloy,” *Int. J. Adv. Manuf. Technol.*, vol. 107, no. 7–8, pp. 3145–3154, 2020, doi: 10.1007/s00170-020-05071-w.

[5] S. Goreczny *et al.*, “Comparison of self-expandable and balloon-expanding stents for hybrid ductal stenting in hypoplastic left heart complex,” *Cardiol. Young*, vol. 27, no. 5, pp. 837–845, 2017, doi: 10.1017/S1047951116001347.

[6] W. G. Choi *et al.*, “Study design and rationale of the ‘Balloon-Expandable Cobalt Chromium SCUBA Stent versus Self-Expandable COMPLETE-SE Nitinol Stent for the Atherosclerotic ILIAC Arterial Disease (SENS-ILIAC Trial) Trial’: Study protocol for a randomized controlled trial,” *Trials*, vol. 17, no. 1, pp. 1–10, 2016, doi: 10.1186/s13063-016-1435-9.

[7] A. Cremonesi, F. Castriota, G. G. Secco, S. Macdonald, and M. Roffi, “Carotid artery stenting: An update,” *Eur. Heart J.*, vol. 36, no. 1, pp. 13–21, 2015, doi: 10.1093/eurheartj/ehu446.

[8] G. Song, H. Q. Zhao, Q. Liu, and Z. Fan, “Bioactive Materials A review on biodegradable biliary stents : materials and future trends,” *Bioact. Mater.*, vol. 17, no. February, pp. 488–495, 2022, doi: 10.1016/j.bioactmat.2022.01.017.

[9] R. Mehrabi, M. T. Andani, M. Elahinia, and M. Kadkhodaei, “Anisotropic behavior of superelastic NiTi shape memory alloys; an experimental investigation and constitutive modeling,” *Mech. Mater.*, vol. 77, pp. 110–124, 2014, doi: 10.1016/j.mechmat.2014.07.006.

[10] R. Madhkour, A. Wahl, F. Praz, and B. Meier, “Amplatzer patent foramen ovale occluder: safety and efficacy,” *Expert Rev. Med. Devices*, vol. 16, no. 3, pp. 173–182, 2019, doi: 10.1080/17434440.2019.1581060.

[11] K. Bishu and E. J. Armstrong, “Supera self-expanding stents for endovascular treatment of femoropopliteal disease: A review of the clinical evidence,” *Vasc. Health Risk Manag.*, vol. 11, pp. 387–395, 2015, doi: 10.2147/VHRM.S70229.

[12] K. Subramaniam, A. Ibarra, and M. L. Boisen, “Echocardiographic Guidance of AMPLATZER Amulet Left Atrial Appendage Occlusion Device Placement,” *Semin. Cardiothorac. Vasc. Anesth.*, vol. 23, no. 2, pp. 248–255, 2019, doi: 10.1177/1089253218758463.

[13] M. E. Seigerman, A. Nathan, and S. Anwaruddin, “The Lotus Valve System: an In-depth Review of the Technology,” *Curr. Cardiol. Rep.*, vol. 21, no. 12, pp. 1–9, 2019, doi: 10.1007/s11886-019-1234-5.

[14] M. R. Jedwab and C. O. Clerc, “A study of the geometrical and mechanical properties of a self-expanding metallic stent--theory and experiment.,” *J. Appl. Biomater.*, vol. 4, no. 1, pp. 77–85, 1993, doi: 10.1002/jab.770040111.

[15] C. Shanahan, P. Tiernan, and S. A. M. Tofail, “Looped ends versus open ends braided stent: A comparison of the mechanical behaviour using analytical and numerical methods,” *J. Mech. Behav. Biomed. Mater.*, vol. 75, no. February, pp. 581–591, 2017, doi: 10.1016/j.jmbbm.2017.08.025.

[16] C. Pan, Y. Han, and J. Lu, “Structural design of vascular stents: A review,” *Micromachines*, vol. 12, no. 7, pp. 1–26, 2021, doi: 10.3390/mi12070770.

[17] J. C. Bansal, “Particle swarm optimization,” *Stud. Comput. Intell.*, vol. 779, no. 3, pp. 11–23, 2019, doi: 10.1007/978-3-319-91341-4_2.

[18] D. Stoeckel, C. Bonsignore, and S. Duda, “A survey of stent designs,” *Minim. Invasive Ther. Allied Technol.*, vol. 11, no. 4, pp. 137–147, 2002, doi: 10.1080/136457002760273340.

[19] J. Mohd, M. Leary, A. Subic, and M. A. Gibson, “A review of shape memory alloy research , applications and opportunities,” *Mater. Des.*, vol. 56, pp. 1078–1113, 2014, doi: 10.1016/j.matdes.2013.11.084.

[20] A. Zaccaria, G. Pennati, and L. Petrini, “Analytical methods for braided stents design and comparison with FEA,” *J. Mech. Behav. Biomed. Mater.*, vol. 119, no. January, p. 104560, 2021, doi: 10.1016/j.jmbbm.2021.104560.

[21] M. Liu, Y. Tian, J. Cheng, Y. Zhang, G. Zhao, and Z. Ni, “Journal of the Mechanical Behavior of Biomedical Materials Mixed-braided stent : An effective way to improve comprehensive mechanical properties of poly (L-lactic acid) self-expandable braided stent,” *J. Mech. Behav. Biomed. Mater.*, vol. 128, no. January, p. 105123, 2022, doi: 10.1016/j.jmbbm.2022.105123.

[22] M. De Beule *et al.*, “FINITE ELEMENT ANALYSIS OF SELF EXPANDING BRAIDED WIRE 2 . MATERIALS AND METHODS,” 2011.